Iraqi Journal of Physics, 2025
https://doi.org/10.30723/ijp.v23i4.1347

Vol.23, No.4, PP.17-27
P-ISSN: 2070-4003
E-ISSN: 2664-5548

Non- Resonant Reaction Rate for ^{15}N (p,γ)^{16}O Reaction

Fatimah Fadhil Abd Ali[1*] and Ahmed Abdul-Razzaq Selman[2]
[1]*Department of Medical Physics, College of Science, Al-Nahrain University, Baghdad, Iraq*
[2]*Department of Astronomy and Space, College of Science, University of Baghdad, Baghdad, Iraq*
[*]Corresponding author: fatima.abd21041a@sc.uobaghdad.edu.iq

Abstract

Light isotopes, especially closed-shell nuclei, have significance in thermonuclear reactions of the Carbon-Nitrogen-Oxygen (CNO) cycle in stars. In this research, radiative proton capture of $^{15}N(p,\gamma)^{16}O$ was calculated using MATLAB codes to find the reaction rate across a temperature range up to 10 GK for the spectrum's non-resonant part, and the astrophysical S- factor S(E) only at low energies (E=70 keV). The findings were compared with conventional reactions before and after statistical analyses, and the results were acceptable when compared to earlier compilations and reference libraries. For temperatures $0.07 < T_9 < 0.09$, current direct data cover 50-90 % of the region under the Gamow peak. At $T_9 < 0.15$, non-resonant capture becomes more important, and the current rate is up to 40 % lower than NACRE-II due to lower S factor values than the NACRE-II extrapolation. For energies E < 70 keV, a linear relationship for the S-factor was assumed.

Article Info.

Keywords:
Gamow Energy, Nucleosynthesis, Radiative Capture Reactions, S-Factor, Reaction Rates.

Article history:
Received: Oct. 13, 2024
Revised: Nov. 06, 2024
Accepted: Nov. 23, 2024
Published:Dec. 01, 2025

1. Introduction

Nucleosynthesis heavily depends on radiative capture reactions. Light elements are formed during fusion reactions in stellar cores or from the Big Bang. In the latter scenario, they are produced mainly by fusion, distinguished by two key chemical sequences: (i) the proton-proton (pp) chain and (ii) the Carbon, Nitrogen, and Oxygen (CNO) cycle [1]. Also, the triple alpha fusion reaction plays quite an important role in changing the chemical elements of the cosmos. The CNO cycle, a catalytic process, requires a high starting concentration of carbon, nitrogen, and oxygen in stellar material. Nuclear astrophysics depends on radiation capture processes, which require the fusion of an atomic nucleus with a proton or neutron to create electromagnetic radiation or α-particles [2, 3]. The CNO cycle mechanism relies heavily on competing p,γ and p,α reactions [1]. The strong connection p,α branches outperform the electromagnetic p,γ branches. However, in some situations, the latter can be equivalent to the p, α branch, significantly affecting the reaction flow in some astrophysical temperature regimes [4].

The initial mass of a star affects whether it burns via the proton-proton (pp) chain or the CNO cycle, which fuses hydrogen to helium via a series of thermonuclear events, providing the bulk of the energy emitted by hot stars [5,6]. Unlike the pp chain, the CNO cycle is a catalytic cycle in which four protons combine with pre-existing carbon, nitrogen, and oxygen seed isotopes to generate one helium nucleus. The carbon, nitrogen, and oxygen isotopes act as independent catalysts in the CNO cycle. However, the second branch of the CNO cycle involves the seed isotopes of oxygen and fluorine, which are

mostly converted into ^{14}N. The fluorine created in this branch is only an intermediate product and does not accumulate in the star in a steady state. The CNO bi-cycle includes the following sequences of nuclear reactions:

$$^{12}C(p,\gamma)^{13}N(\beta^+\nu)^{13}C(p,\gamma)^{14}N(p,\gamma)^{15}O(\beta^+\nu)^{15}N \rightarrow ^{15}N(p,\alpha)^{12}C \rightarrow ^{15}N(p,\gamma)^{16}O(p,\gamma)^{17}F(\beta^+\nu)^{17}O(p,\alpha)^{14}N \quad \textbf{(1)}$$

The CNO bi-cycle, often known as the "cold" CNO cycle, produces three electron neutrinos through beta decays of ^{13}N, ^{15}O, and ^{17}F [7]. The CN cycle lacks stable ^{13}N and ^{15}O isotopes of nitrogen and oxygen, which decay to the stable isotopes ^{13}C and ^{15}N, respectively. The enter reaction ^{15}N(p,γ)^{16}O removes catalytic nuclei from the process. Reactions that follow in (1) restore the catalytic material, resulting in the buildup of ^{16}O and heavier isotopes, including ^{4}He and ^{14}N nuclei. This second branch generates ^{17}F, which decays, emitting beta rays and 1.74 MeV electron neutrinos. The ^{15}N(p,γ)^{16}O mechanism links the alternate NO channel of the CNO cycle, resulting in stable oxygen isotopes. In the CNO cycle, the proton capture process on ^{15}N can occur through two channels: ^{15}N (p,^{4}He)^{12}C and ^{15}N(p,γ)^{16}O reactions, which meet at the ^{15}N nucleus. The rate of CN with regard to the NO cycle is determined by the branching ratio of the ^{15}N(p,γ)^{16}O and ^{15}N(p,α)^{12}C reaction cross sections. The ^{15}N (p,γ)^{16}O process has a low likelihood of Occurrence probability and has a significant impact on nucleosynthesis [8]. However, its contribution to overall nuclear energy generation is modest [9]. To accurately forecast the abundances and relative ratios of stable ^{16}O, ^{17}O, and ^{18}O isotopes in an active NO cycle, the ^{15}N(p,γ)^{16}O reaction must be correctly evaluated [10-12]. The reaction rate ratio defines how much nucleosynthesis of ^{16}O, ^{17}O, and ^{18}O occurs during CNO combustion [10]. The ^{15}N(p,γ)^{16}O reaction (Q-value 12.127 MeV) is important in the combustion of CNO hydrogen in novae and AGB stars. The ^{15}N (p,γ)^{16}O reaction is impacted at stellar energies by two interfering resonances at $E_R = 312$ keV($J^\pi = 1^-$) and $E_R = 964$ keV($J^\pi = 1^-$), where E_R is the resonance energy in the center of mass (CM) system [13,14]. Hebbard [13] used a sodium iodide detector to study this reaction in 1960, while Rolfs and Rodney [14] used a Ge(Li) detector in 1974. Only the most recent result is included in the NACRE compilation [15]. At low energies, there is a difference in the findings of the two experiments, as well as in the extrapolated S-factors ($S(0)_{Hebbard} = 29.8 \pm 5.4$ keV . b whereas $S(0)_{Rolfs} = 64.0 \pm 6.0$ keV. b).

Coulomb barrier dominates at low energies in the non-resonance positively charged particle-induced reaction due to the positive charge of the reactants. To fuse such particles, they must first break through their mutual repulsive Coulomb barrier U_0 and move apart far enough (about 10^{-15}m, which is a typical nuclear size) for the strong nuclear force to take over. A difference was discovered when the energy needed to fuse two hydrogen atoms at r = 1 fm, where it was computed and put up against the Sun's average particle kinetic energy of 3/2 kT [16]. It was discovered that a temperature of 10^{10} K is the minimal requirement for the fusion process. However, temperature in the Sun's center is just 1.6×10^7 K. As a result, the Sun's core's temperature is insufficient for nuclei to break through the Coulomb barrier .

Sometimes, there are a preferred set of conditions for a nuclear reaction to occur, such as matching between incident particle energy with an excited state level, or spin matching between incident and target nucleus… etc. In such cases, the reaction cross section increases rapidly at specific region (s) of reaction energy so the measured cross

section appears to fluctuate. This phenomenon is called nuclear resonance. The reasons behind the nuclear resonance phenomenon are not simple in general. But when it happens, nuclear resonance brings many important effects. It can cause absorption of incident particles at an extremely higher rate at a selective energy and generates certain abundant products as well. Usually, resonance occurs at low incident energies. Thus it is important to consider its effects when addressing thermonuclear and capture reactions [17].

The aim of the present work is to study the thermonuclear reaction rates for the most significant CNO cycle reactions at stellar temperatures from (10^7 to 10^9) K by focusing on specific samples of massive stars with the CNO cycle. Then, a comparison was made for the model calculations with data from available compilations and libraries. Furthermore, the best probability distribution functions that govern the rate of these reactions was found. A MATLAB computer code was used to perform the analysis, and the results were compared with the available experimental data of NACRE [European Nuclear Astrophysics Compilation of Reaction Rates].

2. Thermonuclear Reaction Rates

A Maxwell-Boltzmann distribution effectively approximates nuclear velocities under sunny circumstances [7]. Therefore, The Maxwell distribution also applies to the relative velocity distribution. The Boltzmann constant, which is regulated by the decreased mass of colliding nuclei, is estimated from the equation [18, 19]:

$$\langle \sigma v \rangle = \left(\frac{8}{\pi\mu}\right)^{\frac{1}{2}} (kT)^{-\frac{3}{2}} \int_0^\infty E\, \sigma(E)\, e^{-\frac{E}{kT}} dE \qquad (2)$$

where μ is the reduced mass of the entrance channel, k is Boltzmann constant, σ is the reaction cross section and E is the center-of-mass energy between the reacting particles. The cross-section, in most cases has a combined contribution from both non-resonant and resonance components. In this work non-resonant contribution were determined as follows: Considering charged-particle induced reactions, the cross section σ (E) can be expressed as [18]:

$$\sigma(E) = S(E)/Ee^{-2\pi\eta} \qquad (3)$$

where S(E) is the astrophysical S-factor and is determined by the equation:

$$\eta(E) = \frac{Z_1 Z_2 e^2}{\hbar v} = 0.1575\, Z_1 Z_2 \left(\frac{\mu}{E}\right)^{\frac{1}{2}} \qquad (4)$$

$\eta(E)$ is the Sommerfeld parameter, Z_1 and Z_2 are the interacting nuclei's charge numbers, and h is the reduced Planck constant. In the absence of resonances, the S-factor is a significantly smoother function of energy than the cross section [19]; it corresponds to a simple quantum tunneling model and the actual cross section of the reaction. This is accomplished by accounting for all of the contributions of the internal structure of the reacting nuclei to the σ (E):

$$N_A\langle \sigma v \rangle = N_A \left(\frac{8}{\pi\mu}\right)^{\frac{1}{2}} (kT)^{-\frac{3}{2}} \int_0^\infty S(E)\, e^{-2\pi\eta} e^{-\frac{E}{kT}}\, dE \qquad (5)$$

The integral part of the reaction rate equation, Eq. (5), is governed by a combined effect of two exponential terms: the first represents the Maxwell Boltzmann (M.B.)

distribution ($e^{-E/kT}$) and the second reflects the Gamow factor ($e^{-1/\sqrt{E}}$) found in Sommerfeld term (Eq.3), and each of them is interestingly energy-dependent, with $e^{-1/\sqrt{E}}$ proportionally to E and $e^{-E/kT}$ inversely with E .As a result, the integral largest contribution must originate from energies where the product of both elements is near maximal. This area is known as the Gamow window (at integral's largest contribution), and it reflects the relatively small energy range in plasma of a star where most of the non-resonant thermonuclear events occur [19, 20]. This window's effective width is [19]:

$$\Delta = 0.2368\ (Z_1^2\ Z_2^2\ \mu\ T_9^5)^{\frac{1}{6}} \quad \text{MeV} \tag{6}$$

Centered around an energy E_0:

$$E_0 = 0.122\ (z_1^2 z_2^2 \mu\ T_9^2)^{1/3} \quad \text{MeV} \tag{7}$$

This gives the effective mean energy for thermonuclear reaction at a given temperature T. Eq. (5) is expressed in terms of the Astrophysical Spectroscopic S-Factor, S(E), rather than the cross section, because the latter is strongly dependent on the reaction energy in most reactions. The S-factor is supplied for a variety of processes; however, at effective stellar temperatures, it is more practical to incorporate the Effective S-Factor, S_{eff} [18], into Eq. (2). It is usual to theoretically describe S_{eff} by terms of Taylor expansion about a specific energy E=0. The factor $e^{-2\pi\eta}$ approximates the permeability of the Coulomb barrier between two point-like particles with charge eZ_1 and eZ_2.

$$S_{eff} = S(0)\left[1 + \frac{5}{12\tau} + \frac{\dot{S}(0)}{S(0)}\left(E_0 + \frac{35}{36}kT\right) + \frac{1}{2}\frac{\ddot{S}(0)}{S(0)}\left(E_0^2 + \frac{89}{36}E_0 kT\right)\right] \tag{8}$$

The dot represents derivative of S(E) with respect to energy *E*. Usually, each of the terms $S(0)$, $\dot{S}(0)$, and $\ddot{S}(0)$ are obtained from fitting experimental data. These terms are the first three terms from Taylor expansion of S(E) around E=0. When the energy and σ are, given in MeV and barns, respectively, then: $S(0)$, $\dot{S}(0)$, and $\ddot{S}(0)$ are given in unit of (MeV. barn), (barn), and (barn/ MeV), respectively. τ is a dimensionless correction parameter described as:

$$\tau = \frac{3E_0}{kT} = 4.2487(Z_1^2\ Z_2^2\ \mu/T_9)^{1/3} \tag{9}$$

$$F(\tau) \approx 1 + \frac{5}{12\tau} \tag{10}$$

This correction has little effect at low temperatures, but its effect is shown to rise with rising temperature, resulting in a decrease in the Coulomb barrier effect.
The final form of the non-resonant reaction rate is [20]:

$$N_A\langle\sigma v\rangle_{Non.R.} = \frac{4.339 \times 10^8}{Z_0 Z_1}\frac{m_0 + m_1}{m_0 m_1} S_{eff}\ e^{-\tau}\ \tau^2 \tag{11}$$

In Eq. (8), t is a numeric factor that corresponds to the atomic numbers of the target and projectile [21], and the S-factor values are treated as temporal derivatives. Z_1 and Z_2

are the atomic numbers of the projectile and target parties, respectively. A few other adjustments might be considered when inserting Eq. (8) into Eq. (5), such as screening effects and non-symmetry of the Gamow window [22, 23].

3. Screening Effect: Reaction Rate Enhancement Factor

This is a minor correction that contributes less than 2-5%, which is included in this work to obtain better agreement of standard experimental with theoretical data. The numerical formula for reaction rate, Eq. (1), is often calculated assuming pure electrostatic contact between two bare, unscreened nuclei. However, in stellar interiors, where temperatures and densities are high, reactant nuclei are enveloped in a spherically symmetric, negatively charged cloud of free electrons that serves as a screening potential for projectiles against the Coulomb repulsive barrier. This produces an effect comparable to that produced using atomic orbital electron screening [24].

Shielding reduces the incoming projectile's Coulomb barrier potential by a certain amount, increasing the reaction cross-section and modifying the penetration factor.
The screened reactivity of a charged particle-induced reaction is typically a product of the ordinary stellar reactivity $\langle\sigma v\rangle$ and the screening enhancement factor $F(E)$:

$$\langle\sigma v\rangle_{\text{screened}} = F(E)\,\langle\sigma v\rangle \qquad (\mathbf{12})$$

with

$$F(E) = \frac{\sigma_s(E)}{\sigma_b(E)} = \frac{\sigma_b(E + U_e)}{\sigma_b(E)} \qquad (\mathbf{13})$$

$$F(E) \approx \exp\left(\pi\eta(E)\frac{U_e}{E}\right) \qquad (\mathbf{14})$$

where σ_s and σ_b are the screening and bare nuclei cross sections at center-of-mass energy E, respectively, and η is the Sommerfeld parameter.

4. Results and Discussion

The cross-section, which in most circumstances contains a cumulative contribution from non-resonant and resonant components, provides the foundation for establishing any stellar reaction rate. Modelling of the non-resonant component of the charged-particle-induced reaction (p,γ) was performed using the Matlab program. The program utilizing Eq. (11) to calculate the non-resonant reaction rates depends on the values of the S-factor coefficient. The non-resonant contribution to charge particle-induced reactions highly depends on temperature and target-projectile charge. It is clear from Table (1) that, at a constant temperature, the entrance channel with a higher atomic number has a greater Coulomb potential($U_0 \propto Z_0 Z_1$). As a result, the reaction probability shifts to a higher temperature area to give the necessary energy for the projectile to cross the Coulomb barrier and produce a reaction. This explains why light nuclei provide most nuclear energy in star plasma rather than heavy ones [21]. The numerical values of reaction rate results are presented in Table 1 for $^{15}N(p,\gamma)^{16}O$ reaction. These data were obtained directly from the websites [25], where the temperature T_9 is given in GK (1 GK=10^9 Kelvins). Therefore, T_9=1.0 indicates T=10^9 K, and the reaction rates are given in $cm^3\ mol^{-1}\ sec^{-1}$. In this research, numerical calculations were made for the selected reaction, and then Compared to the numerical results in Table (1) for the nuclear reaction $^{15}N(p,\gamma)^{16}O$ at temperature $0.007 \leq T_9 \leq 10$ GK for $S(0) = 45 \times 10^6$ MeV. b ($\pm$ 9 keV. b, obtained from NACREE-

II[25] and Q-value +12.127 MeV [24,26].The comparison showed a good agreement with the theoretical calculation. This result indicates that the light nuclei generate more energy in the stellar plasma than the heavy nuclei. The results show that the thermonuclear reaction rate increased as temperatures rose because charged interacting particles needed more temperature to pass through the existing Coulomb barrier.

Fig.1 shows the relationship between the S_{eff} and temperature T_9 in GK. The S-factor coefficients were selected from libraries to compute S_{eff} values. Then, S_{eff} was calculated using Matlab code, depending on the coefficients S(0) from Eq. (8), and then utilized to estimate the non-resonant rates for $^{15}N(p,\gamma)^{16}O$ reaction, as listed in Table 1, because the Coulomb barrier must be overcome by charged interacting particles as the temperature increases for $^{15}N(p,\gamma)^{16}O$ reaction in intermediate and massive stars, the results showed that the S_{eff} increased as the temperature increased.

Table 1: The numerical values of $^{15}N(p,\gamma)^{16}O$ reaction rate from European Nuclear Astrophysics Compilation of Reaction Rates ($N_A\langle\sigma v\rangle$ EXP) [from NACRE-II] [25] and calculated by Matlab ($N_A\langle\sigma v\rangle$ THE). Temperature given in (GK = $1\times 10^9 K$), and $N_A\langle\sigma v\rangle$ are in $cm^3 mol^{-1}\ sec^{-1}$.

T_{GK}	$N_A\langle\sigma v\rangle$ [25]	THE.$N_A\langle\sigma v\rangle$	T_{GK}	[25]$N_A\langle\sigma v\rangle$	THE.$N_A\langle\sigma v\rangle$
0.007	4.54×10^{-25}	4.485×10^{-25}	0.18	7.00×10^{-3}	4.1×10^{-3}
0.008	1.34×10^{-23}	1.32×10^{-23}	0.2	1.88×10^{-2}	1.09×10^{-2}
0.009	2.34×10^{-22}	2.30×10^{-22}	0.25	1.48×10^{-1}	1.09×10^{-1}
0.01	2.75×10^{-21}	2.70×10^{-21}	0.3	7.72×10^{-1}	6.34×10^{-1}
0.011	2.36×10^{-20}	2.31×10^{-20}	0.35	2.95	1.98
0.012	1.59×10^{-19}	1.55×10^{-19}	0.4	8.85	7.52
0.013	8.73×10^{-19}	8.48×10^{-19}	0.45	2.17×10^{1}	2.01×10^{1}
0.014	4.05×10^{-18}	3.93×10^{-18}	0.5	4.55×10^{1}	4.03×10^{1}
0.015	1.64×10^{-17}	1.60×10^{-17}	0.6	1.41×10^{2}	1.21×10^{2}
0.016	5.86×10^{-16}	5.65×10^{-16}	0.7	3.16×10^{2}	3.09×10^{2}
0.018	5.60×10^{-16}	5.38×10^{-16}	0.8	5.79×10^{2}	5.19×10^{2}
0.02	3.90×10^{-15}	3.73×10^{-15}	0.9	9.30×10^{2}	8.04×10^{2}
0.025	1.91×10^{-13}	1.81×10^{-13}	1	1.37×10^{3}	1.17×10^{3}
0.03	3.70×10^{-12}	3.47×10^{-12}	1.25	2.91×10^{3}	1.31×10^{3}
0.04	2.78×10^{-10}	2.55×10^{-10}	1.5	5.20×10^{3}	4.85×10^{2}
0.05	5.97×10^{-9}	5.38×10^{-9}	1.75	8.35×10^{3}	6.36×10^{3}
0.06	6.21×10^{-8}	5.47×10^{-8}	2	1.23×10^{4}	2.55×10^{3}
0.07	4.03×10^{-7}	3.48×10^{-7}	2.5	2.18×10^{4}	3.28×10^{3}
0.08	1.89×10^{-6}	1.61×10^{-6}	3	3.21×10^{4}	3.99×10^{3}
0.09	6.98×10^{-6}	5.78×10^{-6}	3.5	4.16×10^{4}	3.16×10^{4}
0.1	2.16×10^{-5}	1.78×10^{-5}	4	5.00×10^{4}	4.01×10^{4}
0.11	5.82×10^{-5}	4.59×10^{-5}	5	6.22×10^{4}	3.59×10^{4}
0.12	1.40×10^{-4}	1.07×10^{-4}	6	6.90×10^{4}	5.95×10^{4}
0.13	3.11×10^{-4}	2.32×10^{-4}	7	7.22×10^{4}	6.81×10^{4}
0.14	6.41×10^{-4}	4.57×10^{-4}	8	7.29×10^{4}	8.29×10^{4}
0.15	1.24×10^{-3}	8.45×10^{-3}	9	7.21×10^{4}	9.21×10^{4}
0.16	2.30×10^{-3}	1.5×10^{-3}	10	7.03×10^{4}	9.02×10^{4}

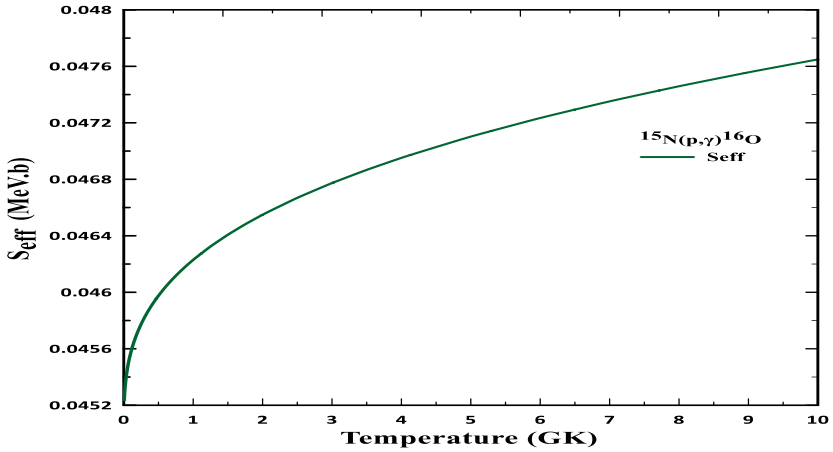

Figure 1: The S_{eff} of $^{15}N(p,\gamma)^{16}O$ as a function of temperature in (GK).

Fig.2 shows the relations between the degree of temperature sensitivity n, and the temperature in GK where n can be calculated as $n = \frac{\tau-2}{3}$ [18]. This means that there is a linear relation between τ and the exponent n. $^{15}N\ (p,\gamma)^{16}O$ reaction showed low temperature sensitivity. As shown in Table 1, the $^{15}N\ (p,\gamma)^{16}O$ reaction reduced faster at low temperatures. However, when the temperature rises, the number density of the reaction's target nuclei experiences a higher consumption rate than (such as $^{13}N\ (p,\gamma)^{14}O$). Furthermore, many poison reactions compete with the $^{15}N(p,\gamma)^{16}O$ channel, as seen in intermediate and massive stars. Furthermore, in this work, two modifications were added to the calculated reaction rate for this reaction. Figs.3 and 4 show the results of the screening corrections vs. T_{GK}. It is noted that the correction factor $F(\tau)$ for the reactions goes into S_{eff} calculations presenting a minimal improvement to the value of rate for the selected temperature range in this work.

S_{eff} values have been calculated using MATLAB code, depending on the coefficients S (0), $\dot{S}(0)$, and $\ddot{S}(0)$through Eq. (8). At low temperatures, the correction factor is often minimal (less than a few per cent). Its magnitude rises with increasing temperature and decreasing Coulomb barrier.

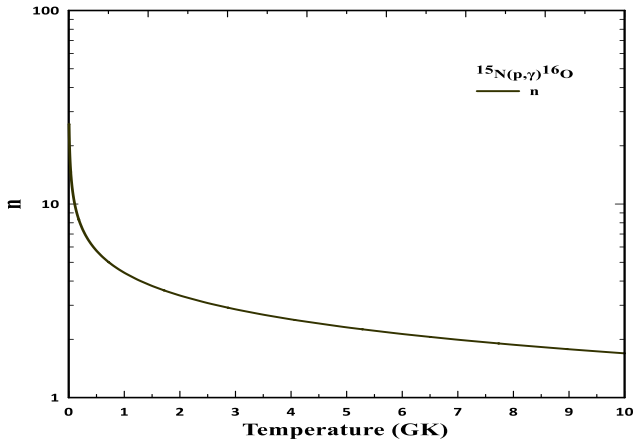

Figure 2: The degree order of reaction temperature sensitivity as a function of temperature in GK for $^{15}N(p,\gamma)^{16}O$ reaction.

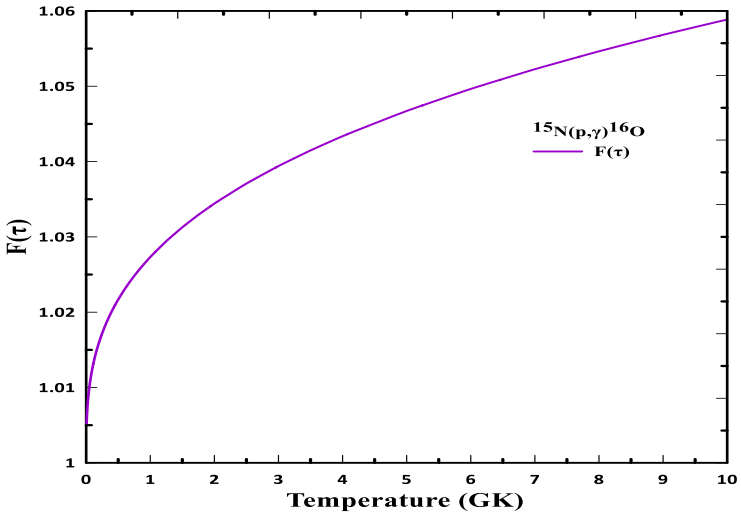

Figure 3: The screening correction factor $F(\tau)$ versus temperature in (GK) for ^{15}N (p,γ)^{16}O reaction.

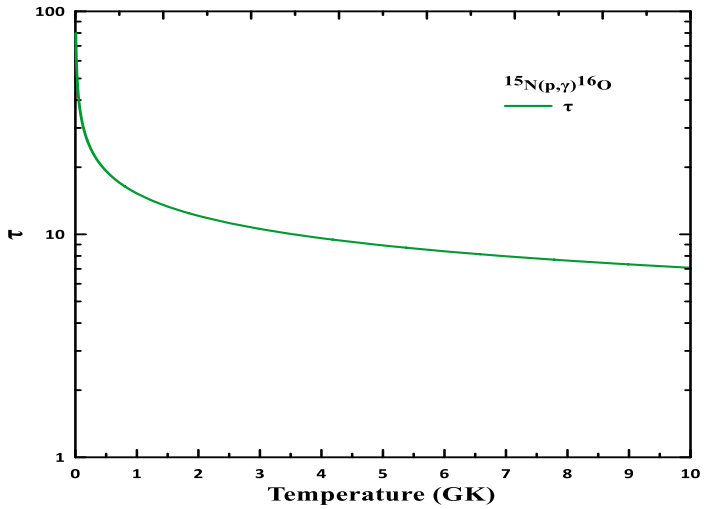

Figure 4: Numerical values of the parameter τ versus temperature in GK for ^{15}N (p,γ)^{16}O reaction.

Fig.5 shows the relation between the reaction rate of ^{15}N (p,γ)^{16}O reaction compared with the present theoretical computed as a function of temperature T_9 using MATLAB. When the temperature rises, the number density of the reaction's target nuclei experiences a higher consumption rate than $^{13}N(p,\gamma)^{14}O$ Furthermore, many poison reactions (such as $^{13}N(p,\gamma)^{14}O$) compete with the $^{15}N(p,\gamma)^{16}O$ channel, making $^{15}N(p,\gamma)^{16}O$ the proton production source, as seen in massive stars and demonstrated that in the region with T_9= 0.09, the shielding effect has a considerable influence on the reaction rate value, especially for targets with a larger atomic number.

However, as the temperature rises, the projectile energy increases, and the projectile goes through the target at such a high velocity that the electrons are unable to protect it from the repulsive Coulomb potential. As a result, the effective screening potential becomes practically constant and has only a minor effect on the response rate value. It was concluded that the increased binding energy of these isotopes makes the reaction less

likely, allowing other competitive processes to arise and increasing the likelihood of other competitive proton reactions in the CNO cycle. This reaction has two significant aspects [27] in the cold CNO cycle: (1) it causes the cold cycle to break down, and (2) its primary energy is supplied from this cycle.

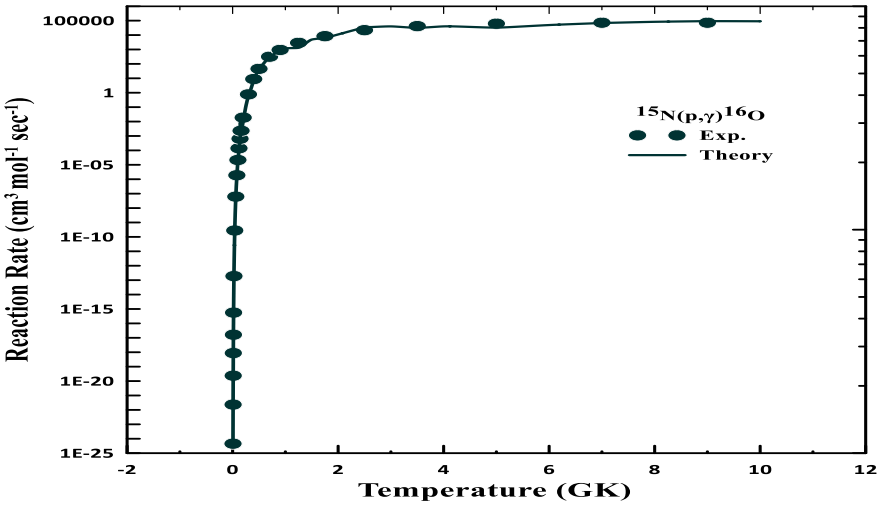

Figure 5: The presently (Theory) calculated non-resonant reaction rate in cm^3 mol^{-1} s^{-1} as a function of temperature in (GK) for $^{15}N(p,\gamma)^{16}O$ compared with (Exp.) values from ref. [25].

5. Conclusions

At T < 0.15 GK, the non-resonance component was found to be the leading component of the total (p, γ) rate values. However, once the temperature exceeded 0.15 GK, the resonance contribution started to play a significant role in the total rate and eventually reached its maximum. The results indicated that Seff increased with rising temperature, which, in turn, led to an increase in the non-resonant reaction rate, as charged interacting particles must overcome the Coulomb barrier at higher temperatures in intermediate- and massive-star interiors.

Conflict of Interest

Authors declare that they have no conflict of interest.

References

1. M. Wiescher, J. Görres, E. Uberseder, G. Imbriani, and M. Pignatari., Annu. Rev. Nucl. Part. Sci. **60**, 381 (2010). https://doi.org/10.1146/annurev.nucl.012809.104505.
2. M. Wiescher, F. Käppeler, and K. Langanke, Annu. Rev. Astron. Astrophys., **50**, 165 (2012). https://doi.org/10.1146/annurev-astro-081811-125543.
3. C. R. Brune and B. Davids, Annu. Rev. Nucl. Part. Sci., **65**, 87 (2015). https://doi.org/10.1146/annurev-nucl-102014-022027.
4. M. Wiescher, H. W. Becker, J. Görres, K.U. Kettner, H.P. Trautvetter, W.E. Kieser, C. Rolfs, R.E. Azuma, K.P. Jackson, and J.W. Hammer, Nucl. Phys., A **349,** 165 (1980). https://doi.org/10.1016/0375-9474(80)90451-0.
5. C. A. Barnes, D. D. Clayton, D. N. Schramm, *Essays in Nuclear Astrophysics*. Presented to William A. Fowler, Cambridge University Press. United Kingdom (1982).
6. M. Arnould and S. Goriely, Prog. Part. Nucl. Phys. **112**, 103766 (2020). https://doi.org/10.1016/j.ppnp.2020.103766.

7. M. Wiescher, J. G¨orres, E. Uberseder, G. Imbriani, and M.Pignatari, Annu. Rev. Nucl.Part. Sci., **60**, 381 (2010). https://doi.org/10.1146/annurev.nucl.012809.104505.
8. A. Boeltzig, C. G. Bruno, F. Cavanna, S. Cristallo, T. Davinson, R. Depalo, R. J. deBoer, A. Di Leva, F. Ferraro, G. Imbriani, P. Marigo, F. Terrasi, and M. Wiescher, Eur. Phys. J., A **52**, 75 (2016). https://doi.org/10.1140/epja/i2016-16075-4.
9. A. Caciolli, C. Mazzocchi, V. Capogrosso, D. Bemmerer, C. Broggini, P. Corvisiero, H. Costantini, Z. Elekes, A. Formicola, Z. Fülöp, G. Gervino, A. Guglielmetti, C. Gustavino, G. Gyürky, G. Imbriani, M. Junker, A. Lemut, M. Marta, R. Menegazzo, S. Palmerini, P. Prati, V. Roca, C. Rolfs, C. R. Alvarez, E. Somorjai, O. Straniero, F. Strieder, F. Terrasi, H. P. Trautvetter, and A. Vomiero, Astron. Astrophys., A **66**, 533 (2011). https://doi.org/10.1051/0004-6361/201117475.
10. G. R. Caughlan and W. A. Fowler, Astrophys. J., **136**, 453 (1962). https://doi.org/10.1086/147399.
11. M. J. Harris, W. A. Fowler, G. R. Caughlan, and B. A. Zimmerman, ,Ann. Rev. Astron. Astrophys., **21**, 165 (1983). https://doi.org/10.1146/annurev.aa.21.090183.001121.
12. G. R. Caughlan and W. A. Fowler, Atomic Data and Nucl. Data Tables **40**, 283 (1988). https://doi.org/10.1016/0092-640X(88)90009-5.
13. D. Hebbard, Nucl. Phys., **15**, 289 (1960). https://doi.org/10.1016/0029-5582(60)90308-4.
14. C. Rolfs and W. S. Rodney, Nucl. Phys., A **235**, 450 (1974). https://doi.org/10.1016/0375-9474(74)90205-X.
15. C. Angulo, M. Arnould, M. Rayet, P. Descouvemont, D. Baye, C. L.Willain, A. Coc, S. Barhoumi , P. Aguer, C. Rolfs, R. Kunz, J.W. Hammer, A. Mayer, T. Paradellis, S. Kossionides, C. Chronidou, K. Spyrou, S. Degl'Innocenti, G. Fiorentini, B. Ricci, and M. L. Rachti, Nucl. Phys., A **656**, 3 (1999). https://doi.org/10.1016/S0375-9474(99)00030-5.
16. K. R. Lang, *Astrophysical Formulae*, 1st ed.; Springer-Verlag, Berlin. Heidelberg, New York, p. 375, (1974).
17. M. Wiescher, J. G¨orres, and H. Schatz, J. Phys. G: Nucl. Part. Phys. **25**, R133 (1999). https://doi.org/10.1088/0954-3899/25/6/201.
18. C. Iliadis, *Nuclear Physics of Stars*, John Wiley & Sons, (2015).
19. C.Angulo, *Experimental tools for nuclear astrophysics*, Springer, Berlin, Heidelberg, p.253, (2009).
20. A. Formicola and G.Imbriani, Europ. Phys. Journal, A **134**, 89 (2019). https://doi.org/10.1140/EPJP%2FI2019-12497-1.
21. L. T. Ali and A. A. Selman, Iraqi J. Sci., **62**, 5 (2021). https://doi.org/10.24996/10.24996/ijs.2021.62.5.36.
22. L. T. Ali, Ph.D. Thesis,University of Baghdad, 2021.
23. A. A. Selman, Iraqi J. Sci., **64**, 5 (2023). https://doi.org/10.24996/ijs.2023.64.5.42.
24. T. Liolios, Phys. Rev., C **63**, 045801(2001). https://doi.org/10.48550/arXiv.nucl-th/0009071.
25. NACRE II Library, Available http://www.astro.ulb.ac.be/nacreii/index.html, (accessed 15th July 2024).
26. Y. Xu, K .Takahashi, S. Goriely, M. Arnould, M. Ohta, and H. Utsunomiya, Nucl. Phys., A **918** (2013). https://doi.org/10.1016/j.nuclphysa.2013.09.007.
27. G. Stasińska, EPE Sci., **54**, 187 (2012). https://doi.org/10.1051/eas/1254003.

معدل التفاعل الغير رنيني لتفاعل $^{15}N(p,\gamma)^{16}O$

فاطمة فاضل عبد علي [1] واحمد عبد الرزاق سلمان[2]
[1] قسم الفيزياء الطبية، كلية العلوم، جامعة النهرين، بغداد، العراق
[2] قسم الفلك والفضاء، كلية العلوم، جامعة بغداد، بغداد، العراق

الخلاصة
تتجسد للنظائر الخفيفة، وخاصة النوى القشرة المغلقة، أهمية في التفاعلات النووية الحرارية لدورة الكربون والنيتروجين والأكسجين (CNO) في النجوم. في هذا البحث، تم حساب التقاط البروتون الإشعاعي لـ $^{15}N(p,\gamma)^{16}O$ عن طريق معدل التفاعل عبر نطاق درجة حرارة يصل إلى 10 جيجا كلفن للجزء الغير رنان من الطيف، بالإضافة إلى العامل الفيزيائي الفلكي S(E) عند الطاقات المنخفضة E=70 كيلو إلكترون فولت. تم إجراء الحسابات باستخدام كود ماتلاب مكتوب. وتمت مقارنة النتائج مع تفاعلات التقليدية قبل وبعد التحليلات الإحصائية، وكانت النتائج مقبولة بالمقارنة مع المجموعات السابقة والمكتبات المرجعية. بالنسبة لدرجات الحرارة $0.07 < T_9 < 0.09$، تغطي البيانات المباشرة الحالية 50-90% من المنطقة تحت قمة جامو. عند $T_9 < 0.15$، يصبح الالتقاط الغير رنيني أكثر أهمية، ويكون المعدل الحالي أقل بنسبة تصل إلى 40% من NACRE-II بسبب انخفاض قيم عامل S مقارنة باستقراء NACRE-II. بالنسبة للطاقات $E < 70$ كيلو إلكترون فولت، افترضنا وجود علاقة خطية للعامل S.

الكلمات المفتاحية: طاقة كامو، عملية التخليق النووي، تفاعلات الالتقاط الاشعاعي، عامل الفيزياء الفلكي S، معدل التفاعل.